ANTIOXIDANTS & REDOX SIGNALING
Volume 8, Numbers 3 & 4, 2006

Forum Original Research Communication

Transcription Regulation in NIH3T3 Cell Clones Resistant to Diethylmaleate-Induced Oxidative Stress and Apoptosis

RAFFAELLA FARAONIO,[1] PAOLA VERGARA,[1] DOMENICO DI MARZO,[1] MARIA NAPOLITANO,[2] TOMMASO RUSSO,[1] and FILIBERTO CIMINO[1]

ABSTRACT

To investigate the molecular mechanisms underlying the induction of cell resistance to oxidative stress, NIH3T3 cell clones (NIH-DEM clones) were isolated and selected for their ability to survive the exposure to diethylmaleate (DEM), a glutathione-depleting agent. The oxidative stress-resistant phenotype of these clones is stable for at least 1 month in the absence of DEM, and includes the resistance also to other apoptosis-inducing stimuli. The expression profile of several antioxidant genes was examined in four of the DEM-resistant clones in the presence and in absence of DEM. The response to the acute exposure to DEM is similar in wild type and DEM-resistant cells, with the exception of the glutathione-*S*-transferase α1 gene, whose expression is highly induced in NIH-DEM clones. However, in the absence of an acute stress, the expression of some genes is higher in DEM-resistant clones than in wild-type cells and the gene expression profile significantly varies among the clones. In particular, glutathione-*S*-transferase α1 and cystine/glutamate transporter mRNAs are increased in NIH-DEM-12. In these cells, the promoters of the two genes drive a stronger transcription than in wild-type cells, and this appears to be dependent on the transcription factor Nrf2. *Antioxid. Redox Signal.* 8, 365–374.

INTRODUCTION

MAMMALIAN CELLS are exposed to a great number of molecules that are, or are able to generate, reactive oxygen species (ROS). ROS are also generated by the cell itself under various physiological conditions to serve as mediators of intracellular signaling (4, 5, 7). In both cases, when the levels of ROS overwhelm the scavenging capacity of the cell, ROS-induced damages provoke either apoptosis or replicative senescence (6, 19, 21). Cells are equipped with a repertoire of protective systems that contrast the deleterious effects of oxidants. The expression of most of these scavenging systems is inducible, and the regulation acts at the level of transcription of the cognate genes. Thus, a sustained induction of expression of one or more of these genes could result in the selection of cells highly resistant to the oxidative stress. According to this, adaptive antioxidant mechanisms have been described for a variety of cells including Chinese hamster fibroblasts (10), murine epithelial cells (14), human leukemia K562 cells (23), and a thymoma cell line (20).

Numerous anticancer drugs act as apoptosis-inducing agents, and in many cases their effects are at least in part a consequence of an oxidative insult. The exposure to oxidants can lead to the selection of resistant clones. This could contribute to the resistance of neoplastic cells to chemotherapy. Furthermore, it has been demonstrated that neoplastic cells produce high levels of ROS, including H_2O_2. This increased intrinsic ROS production in cancer cells may contribute to the emergence of drug-resistant cells (15, 16). On the other hand, there are many normal cells in old subjects, which survive for long time in the presence of oxidative stress. This suggests that they have developed a certain degree of resistance to

[1]Dipartimento di Biochimica e Biotecnologie Mediche, Università di Napoli Federico II; CEINGE biotecnologie avanzate, Napoli, Italy.
[2]Istituto Nazionale dei Tumori "Fondazione Pascale," Napoli, Italy.

ROS. Thus, as in neoplastic transformation, they are expected to be more resistant to apoptosis-inducing drugs than young cells. Therefore, it is of interest to explore the molecular mechanisms leading to the selection of cells resistant to ROS-induced apoptosis.

Cellular defense mechanisms against ROS include different enzymes and various antioxidant molecules. Examples of enzymes are catalase (CAT), superoxide dismutases (SOD), glutathione peroxidases (GPxs) involved in ROS metabolism, as well as phase-2 enzymes such as glutathione *S*-transferases (GSTs), NAD(P)H:quinone oxidoreductase-1 (NQO1), and heme oxygenase (HO-1).

A common *cis*-element present in the promoters of these ROS-inducible genes is the Antioxidant Response Element (ARE) that binds Nrf2, a member of the NF-E2 family of bZIP transcription factors (2, 22). Nrf2 binds to AREs and activates the transcription of cognate genes. Under basal conditions Nrf2 is sequestered in the cytoplasm by Keap, a multidomain cysteine-rich protein bound to the cytoskeleton (1, 11). Oxidants disrupt the Keap-Nrf2 complex, and this results in nuclear accumulation of Nrf2, where it activates the transcription of ARE-containing promoters (3).

In this paper we explored the phenotype of NIH3T3-derived clones (NIH-DEM clones), selected for their resistance to diethylmaleate (DEM), a compound provoking oxidative stress by depleting the cellular storage of GSH, that is one of the major oxidant-scavenging molecules. We found that NIH3T3 clones resistant to DEM-induced apoptosis are also resistant to other apoptotic stimuli, and display various profiles of expression of several genes encoding anti-oxidant proteins. In one of these clones, that survives the growth in the absence of DEM for more than one month, the overexpression of the glutathione-*S*-transferase α1 (GST α1) and of the cystine/glutamate transporter (x-CT) is due to increased nuclear levels of the transcription factor Nrf2.

MATERIALS AND METHODS

Cell culture and treatment

Immortal murine NIH3T3 cells and NIH-DEM clones were maintained in Dulbecco's modified essential medium (DMEM) supplemented with 10% calf serum (ICN), penicillin 10 U/ml, and streptomycin 10 μg/ml at 37°C under 5% CO_2 atmosphere. Before each experiment, cells were subcultured at density of 3×10^6/100 mm diameter dish in complete medium, and incubated overnight at 37°C. Diethylmaleate (DEM, Sigma, St. Louis, MO, USA) was added directly to the culture medium. Etoposide and BSO were from Sigma.

Selection of DEM-resistant clones from NIH3T3 cells (NIH-DEM clones)

To select DEM-resistant clones, NIH3T3 cells were subcultured at density of 3×10^6/100 mm diameter dish in complete medium and cultured for 20–24 h prior to starting the treatment. DEM was added directly to the culture medium at final concentration of 100 μ*M* and cells were incubated at 37°C. After 4 days, the medium was replaced with the standard medium without DEM and the cultures were continued until clones appeared (approximately 3 weeks). DEM-resistant clones were isolated and propagated in culture without DEM. After that clones were assayed for DEM-resistance, one aliquot of cells was maintained continually in presence of 100 μ*M* DEM, while another aliquot was used for the population without DEM.

Terminal deoxynucleotidyl transferase (TdT)-mediated dUTP nick-end labeling (TUNEL) assay

For *in situ* cell death detection, 3×10^6 cells were plated on coverslips 18–20 h before starting treatments. The day after, 100 μ*M* DEM was added to the complete medium and cells were harvested at different times. For this assay, cells on coverslips were fixed in formaldehyde solution (3.7% in PBS) for 30 min at room temperature. DNA fragmentation analysis was performed using terminal deoxynucleotidyl transferase (TdT)-mediated dUTP nick-end labeling (TUNEL) according to the manufacturer's protocol (In situ Cell Death Detection Kit, Roche Molecular Biochemical, Mannheim, Germany). Briefly, samples were incubated in permeabilization solution (0.1% Triton X-100 in 0.1% sodium citrate) for 2 min on ice, and treated with TUNEL reaction mixture for 60 min at 37°C. Cells were washed twice in PBS, stained with DAPI, and analyzed by fluorescence microscopy.

Flow cytometric analysis of apoptosis

For the analysis of apoptosis by annexin V-FITC and propidium iodide (PI), NIH3T3 and NIH-DEM clones were treated with various agents at desired concentration, for different times. The annexin-V FACS analysis was performed according to the manufacturer's protocol (Trevigen, Inc., Gaithersburg, MD, USA). In brief, after treatments the cells were harvested and centrifuged for 10 min at 1100 rpm. The cell pellet was resuspended in 100 μl annexin V incubation buffer containing 10 μl of binding buffer 10× (100 m*M* Hepes pH 7.4, 1.5 *M* NaCl, 50 m*M* KCl, 10 m*M* MgCl2, 18 m*M* CaCl2), 10 μl of PI, 1 μl of FITC-coniugated annexin V, and 79 μl of H_2O. It was then incubated for 15 min at room temperature in the dark. A total of 400 μl of binding buffer 1× was added to each sample, and cells were analyzed using a MOD FIT LT 2.0 software (Mod Fit, Topsham, ME, USA). Annexin V binds to cells that express phosphatidylserine on the outer layer of the cell membrane, and PI stains the DNA of cells with a compromised cell membrane. This allows for the discrimination of live cells (unstained with either fluorochrome) from early apoptotic cells (stained only with annexin V), late apoptotic cells (stained with both annexin V and PI), and necrotic cells (stained with only PI).

RNA preparation and real- time quantitative RT-PCR

Total RNA was isolated from cells using a Qiagen total RNA isolation kit (Qiagen, Valencia, CA, USA). For quantitative real time PCR, cDNAs were synthesized in a Gene AMP PCR system 9700 from 1 μg of total RNA in 20 μl reaction containing 1× RT buffer with $MgCl_2$ 5 m*M*, 10 m*M* DTT, 5 μ*M* random examers, 1 m*M* dNTP, 1 U/μl RNase inhibitor,

and 10 U/µl reverse transcriptase (M-MLV Reverse Transcriptase, GIBCO/BRL, Invitrogen, Carlsbad, CA, USA). The reaction was incubated at 70°C for 10 min and then at 25°C for 10 min, followed by 42°C for 45 min and 99°C for 3 min. Aliquots of cDNA (1/10 of reverse transcription reactions) were used in real time PCRs. SYBR Green-based real time PCR was used to determine cDNA levels. Aliquots of cDNA were amplified in an iCycler iQ Real-Time PCR Detection System (Biorad, Hercules, CA, USA) using iQ™ SYBR Green Supermix (Invitrogen) in triplicate in 25 µl reaction volumes. The sequences of the mouse primer pairs used were:

c-ABL, 5′-GGTATGAAGGGAGGGTGTACCA-3′ and 5′-GTGAACTAACTCAGCCAGAGTGTTGA;
γ-GCreg, 5′-TGCGAAAAAAGTGCCCGT-3′and 5′-TGCATTCCAAAACATCTGGAAA-3′;
GPx4, 5′-TTACTTAAGCCAGCACTGCTGTG-3′ and 5′-CCATGTGCCCGTCGATGT-3′;
MnSOD, 5′-GTCGCTTACAGATTGCTGCCT-3′and 5′-AGGTAGTAAGCGTGCTCCCACA-3′;
Prdx5, 5′-CAGAGTTTGCCAAGAGGAATGTTAA-3′ and 5′-GTTTCACCATTGTAAGCATTGATGT-3′;
GST α1, 5′-CAGGTGGCTCCTAGCTGCA-3′ and 5′-GGTCTGCGCCAGCTTCA-3′;
GST p1, 5′-TTCTCTCTGCACAGCAGCCA-3′ and 5′-AACCACCTCCTCCTTCCAGC;
Nrf2, 5′-GGCCCAGCATATCCAGACA-3′ and 5′-CCAGGGCAAGCGACTCAT-3′;
Keap1, 5′-CCACATCTACGCAGTCGGG-3′ and 5′-ACAGTTGTAACCGCGCTGAT-3′;
x-CT, 5′-TACCTCAACTTTATTACTGAAGAAGTAGA-CAA-3′ and 5′-TGTCAGTACGTAGCCCACTGTGA-3′
HO-1, 5′-GTGATGGAGCGTCCACAGC-3′ and 5′-TGGTGGCCTCCTTCAAGG-3′;
Catalase, 5′-CGTCCCTGCTGTCTCACGTT-3′ and 5′-ATCTCCTATTGGGTTCCCGC-3′;
NQO1, 5′-CCCTCAACATCTGGAGCCAT-3′ and 5′-GCGTAGTTGAATGATGTCTTCTCTGA-3′.

PCR cycling conditions consist of 95°C for 5 min and 40 cycles of 95°C for 15 s and 60°C for 1 min. Expression levels were calculated relative to c-ABL mRNA levels as endogenous control. Relative expression was calculated as $2^{(Ct\ test\ gene - Ct\ c\text{-}ABL)}$ (13).

Plasmid construction and cell transfections

The promoter regions of GST α1 and x-CT gene were isolated by PCR from genomic DNA from NIH3T3 cells. The 5′ flanking regions of GST α1 (from –940 to +41) and x-CT (from −235 to +180) were cloned into PGL3 Basic vector (Promega, Madison, WI, USA). NIH3T3 and NIH-DEM-12 were transfected with reporter plasmids (5 µg) and pRLSV40 encoding *Renilla* luciferase (Promega) (0.5 µg). At 36 h post-transfection, cells were harvested and analyzed for luciferase activity. The luciferase assay was performed with a Dual-Luciferase Reporter assay System (Promega) according to the manufacturer's instructions. The firefly luciferase activity was normalized to *Renilla* internal control luminescence.

Nuclear protein preparation and Western blot analysis

NIH3T3 and NIH-DEM clones were treated with 100 µ*M* DEM for 3 h, washed twice with cold PBS, solubilized at 4°C with 300 µl of lysis buffer [10 m*M* HEPES, 60 m*M* KCl, 1 m*M* ethylenediaminetetraacetic acid (EDTA), 1 m*M* 1,4-dithiothreitol (DTT), 1 m*M* phenylmethylsulfonyl fluoride (PMSF), 1 m*M* Na_3VO_4, 0.2% NP40, and 10 µg/ml aprotinin, leupeptin, and pepstatin] and centrifuged at 2500 rpm for 5 min at 4°C. The nuclear pellet was washed with lysis buffer without NP40 and resuspended in 300 µl of the same buffer. This volume was added to 300 µl of lysis buffer with 30% saccharose and without NP40, and centrifuged at 6,000 rpm for 15 min at 4°C. The nuclear pellet was resuspended in 50 µl of a buffer containing 250 m*M* Tris-HCl pH 8, 60 m*M* NaCl, 1 m*M* DTT, 1 m*M* Na_3VO_4, 1 m*M* PMSF, and 10 µg/ml aprotinin, leupeptin, and pepstatin. To lyse, cellular nuclei were treated with three cycles freezing (−80°C)/defrosting (37°C). Finally, nuclear proteins were obtained by centrifugation at 9500 rpm for 10 min at 4°C. Fifteen micrograms of supernatant from each sample was heated at 95°C for 5 min, separated by electrophoresis on 10% SDS-polyacrylamide and transferred to Immobilon-P transfer membranes (Millipore, Billerica, MA, USA). Membranes were washed and blocked with 5% nonfat dry milk in PBS containing 0.1% Tween-20 at room temperature for 1 h. Nrf1 and Nrf2 levels were analyzed by Western blotting using 1 µg/ml anti-Nrf1 and anti-Nrf2 rabbit polyclonal antibodies (H-285 and H-300, respectively, Santa Cruz Biotechnology, Inc., Santa Cruz, CA, USA) at room temperature for 2 h. After incubation with rabbit horseradish peroxidase-conjugated secondary antibody at room temperature for 30 min, the blots were developed using enhanced chemiluminescence (Amersham, Uppsala, Sweden).

RESULTS

Isolation of NIH3T3 cell clones resistant to diethylmaleate

NIH3T3 cells were exposed for 48 hours to various concentrations of DEM. Percentage of cell survival was calculated by trypan blue exclusion. As shown in Figure 1A, 100 µ*M* DEM is the lowest concentration that induces the death of almost all cells. By using this concentration of DEM, tunel-positive cells were 30% after 5 h of treatment, and 50% after 8 h (Fig. 1B). FACS analysis of cells exposed to 100 µ*M* DEM for 24 h and stained with both annexin V-FITC and propidium iodide (PI) showed that 37% of the cells were annexin V-positive, while 56% were positive to both annexin V and PI.

These results demonstrate that 100 µ*M* DEM induces a massive apoptosis of these cells. However, it was invariably observed that a small number of cells did survive the treatment and, prolonging the culture for 6 days, this led to the generation of clones that were able to grow in the presence of DEM (NIH-DEM clones). Figure 2A shows the growth curves of four of these clones (NIH-DEM-3, NIH-DEM-5, NIH-DEM-12, and NIH-DEM-21), kept in the presence of a medium containing 100 µ*M* DEM. The results of this exper-

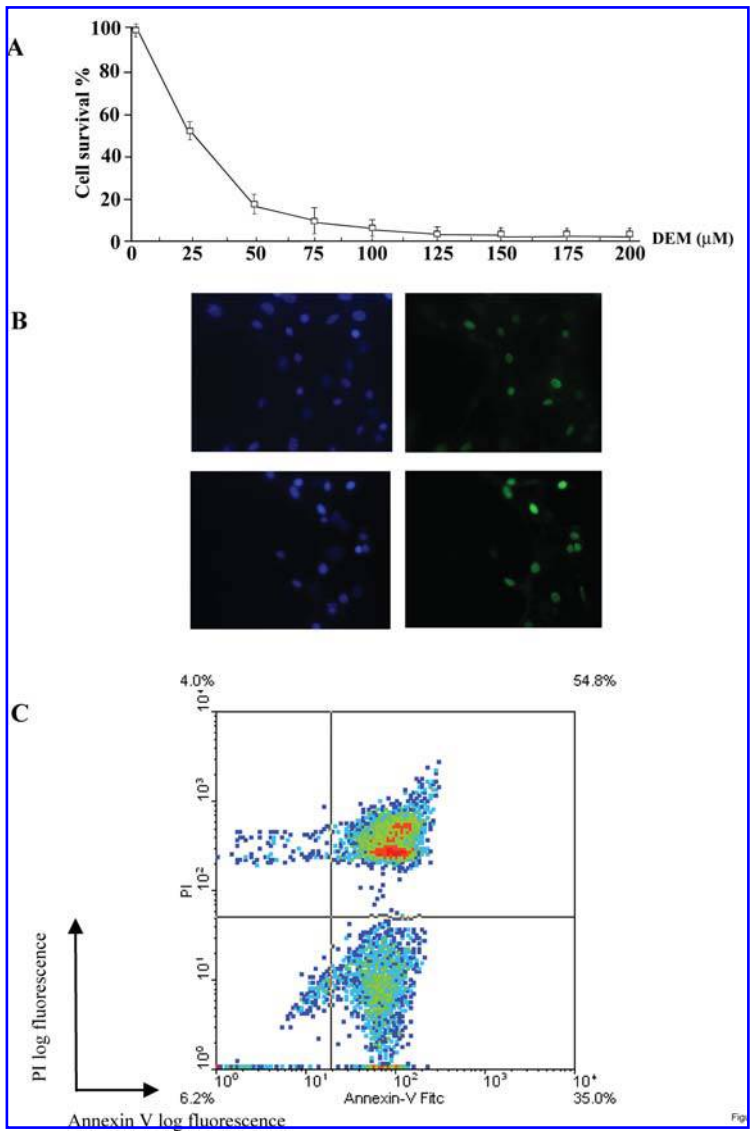

FIG. 1. DEM induces massive apoptosis in NIH3T3 cells. NIH3T3 cells were cultured as described in Materials and Methods for 20–24 h prior to start treatments. DEM was added directly to the medium and cells were incubated at 37°C for different times. (**A**) Percent of surviving cells after 48 h in the medium containing various concentrations of DEM. The main values ± SD of four different measurements of Trypan blue exclusion are reported. (**B**) Staining of apoptotic cells at 5 h (*upper panels*) and 8 h (*lower panels*) was performed by Tunel assay. Cells incorporating the fluorescein (*right*) were counted in several fields and the mean percentage of positive cells was calculated by counting, in the same field, the number of nuclei stained with DAPI (*left*). (**C**). At 24 h apoptosis was detected by annexin V-FITC and PI staining by using FACScan instrument, and the percentages of early apoptotic cells (37.3%, stained only with annexin V), late apoptotic cells (55.8%, stained with both annexin V and PI), and necrotic cells (3%, stained with only PI) was calculated by using a MOD FIT software.

iment show that all the clones were able to grow efficiently in the presence of the drug, although to a lesser extent compared to the wild-type cells kept in the absence of DEM. Furthermore, resistant clones were able to survive in the presence of even higher DEM concentrations, and two of them showed more than 50% of cell survival when exposed for 48 hours to 400 μ*M* DEM (Fig. 2B).

To examine the stability of the phenotype acquired through the selection in 100 μ*M* DEM, the clones were kept in culture various times in the absence of DEM, and then re-exposed to the drug. As shown in Figure 2C, after 1 month in the absence of DEM, a significant number of cells were still resistant to the re-exposure to the drug. Furthermore, aliquots of the clones were harvested and stored at –135°C for 3 months; re-plating the cells in the medium containing 100 μ*M* DEM resulted in the survival of more than 50% of the cells (not shown).

NIH-DEM clones are resistant to various apoptosis-inducing stimuli

To further characterize the phenotype acquired by the NIH-DEM clones, we exposed them to several treatments, which are well known to provoke a massive apoptosis in NIH3T3 cells. First, the cells were treated with another pro-oxidant agent, buthionine sulfoximine (BSO), which induces an accumulation of ROS by inhibiting the GSH synthetase activity (9). As shown in Figure 3B, 24 h treatment with 1 m*M* BSO provoked, in the wild-type NIH-3T3 cells, a massive induction of apoptosis as demonstrated by the accumulation of annexin V-positive cells. On the contrary, this treatment has no significant effects on the NIH-DEM-12 clone. Second, wild-type and NIH-DEM clones were exposed to UV (5 J/m^2 at 254 nm for 10 sec) and analyzed 24 h after irradiation by FACS. Most of the NIH-DEM-12 cells were resistant to UV-

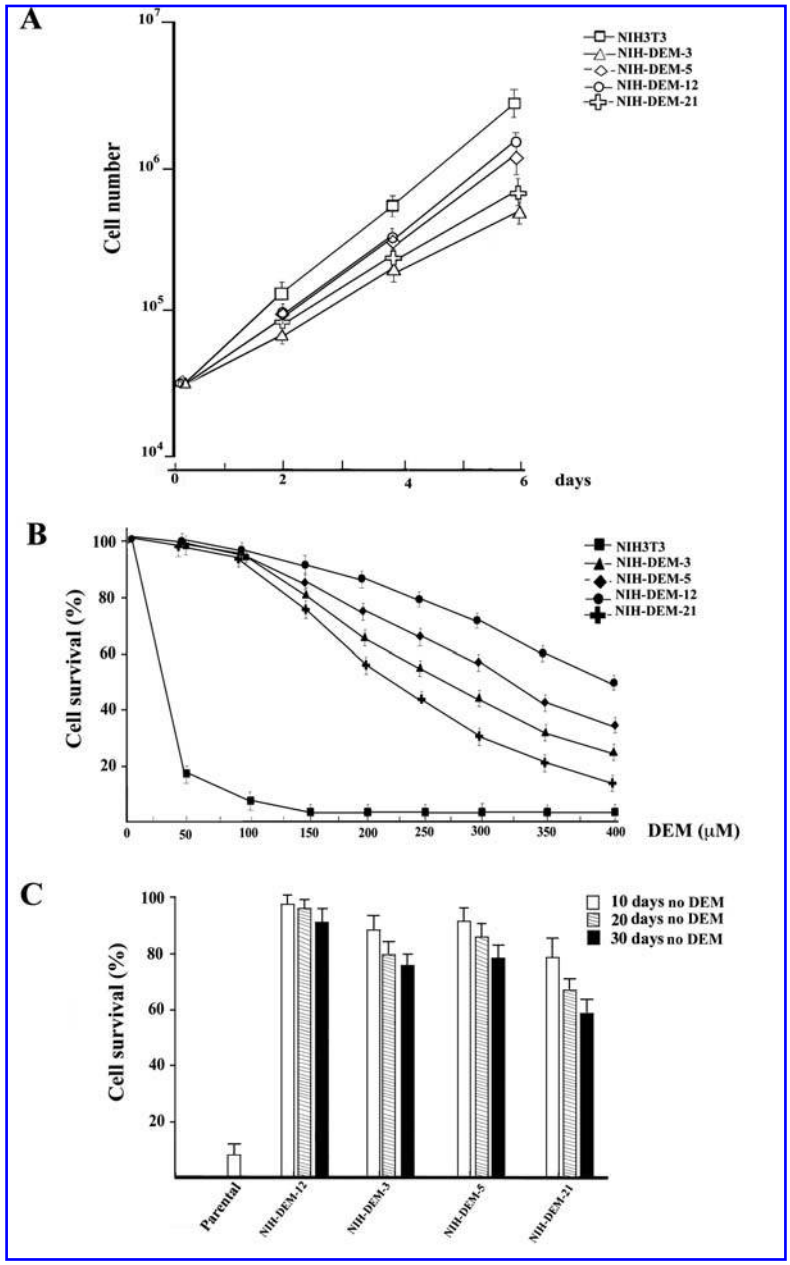

FIG. 2. Growth of NIH-DEM-clones in presence of diethylmaleate (DEM). (**A**) 50 × 10^3 cells of wild-type NIH3T3 or DEM-resistant clones were plated in 100 mm diameter dishes and incubated at 37°C in presence of 100 μ*M* DEM. Cells were trypsinized and counted every 48 h. (**B**) 3 × 10^6 cells were plated in 100 mm diameter dishes and cultured overnight before starting treatments. DEM at different concentrations was added directly to the plates and cells were further cultured at 37°C for 48 h. The numbers of viable cells were measured by XTT assay. Each data point represents the mean of triplicate determinations with error bars indicating standard errors. Cell survival of NIH3T3 parental cell line cultured in presence of DEM is also reported. (**C**). NIH-DEM clones were grown for 10, 20, or 30 days in the absence of DEM, and then exposed to 100 μ*M* DEM for 48 h. Percentage of survival was calculated in triplicate points by trypan blue exclusion assay.

induced apoptosis, showing about 35% of apoptotic cells compared to more than 90% in wild type NIH3T3 (Fig. 3C). Lastly, NIH3T3 and NIH-DEM cells were exposed for 24 h to 150 μ*M* etoposide, that induced a dramatic accumulation of annexin V-positive cells (more than 90%) in wild-type NIH3T3, while only 35% of NIH-DEM became annexin V-positive (Fig. 3D).

NIH-DEM clones show a modified expression of antioxidant-response genes

Several genes are known to be activated after the exposure to oxidative stress (12). We measured the mRNA levels of some of these genes in NIH3T3 cells exposed for 3 h to 100 μ*M* DEM and found that six of these genes, namely glutathione *S*-transferase (GST α1) (a), cystine/glutamate transporter (x-CT) (b), manganese superoxide dismutase (MnSOD) (c), γ-glutamylcysteine synthetase regulatory (GCreg) (e), glutathione *S*-transferase p1 (GST p1) (f), NAD(P)H:quinone oxidoreductase-1 (NQO1) (i), and heme oxygenase (HO-1) (j), are robustly overexpressed. Four of the isolated NIH-DEM clones grown in the presence of 100 μ*M* DEM showed an expression profile similar to that of wild-type cells transiently exposed to the drug, while the expression of glutathione *S*-transferase α1 gene increased more than 50-fold in one clone and more than 120-fold in other three lines (Fig. 4A).

We then examined the expression levels of these genes in the NIH-DEM clones kept for 1 month in the normal medium not supplemented with DEM. As shown in Figure 4B, the ex-

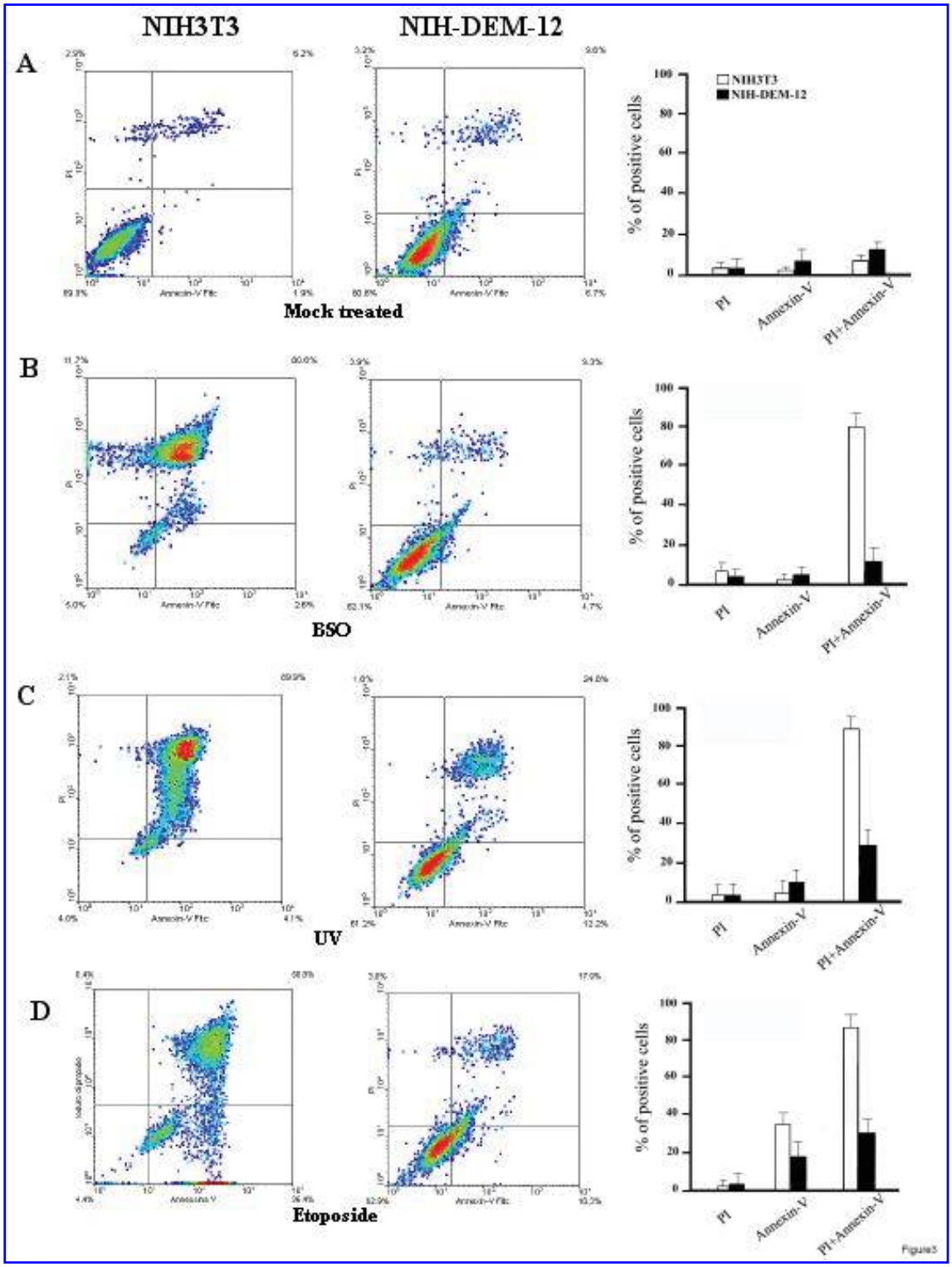

FIG. 3. Resistance to apoptosis of NIH-DEM-12. NIH3T3 cells and NIH-DEM-12 were plated at a density of 3×10^6 cells per dish of 100 mm and incubated overnight at 37°C. Cells were exposed to various apoptotic stimuli: (**A**) none; (**B**) 1 m*M* BSO for 24 h; (**C**) UV radiation (5 J/m^2 at 254 nm for 10 sec), and then cultured for 24 h; (**D**) 150 μ*M* etoposide for 24 h. Cells were then stained with annexin V-FITC and PI and apoptosis was analyzed by FACScan by using a MOD FIT software. The % of positive cells to PI, Annexin-V and PI+ Annexin-V of NIH3T3 (*empty columns*) and NIH-DEM-12 (*filled columns*) are reported.

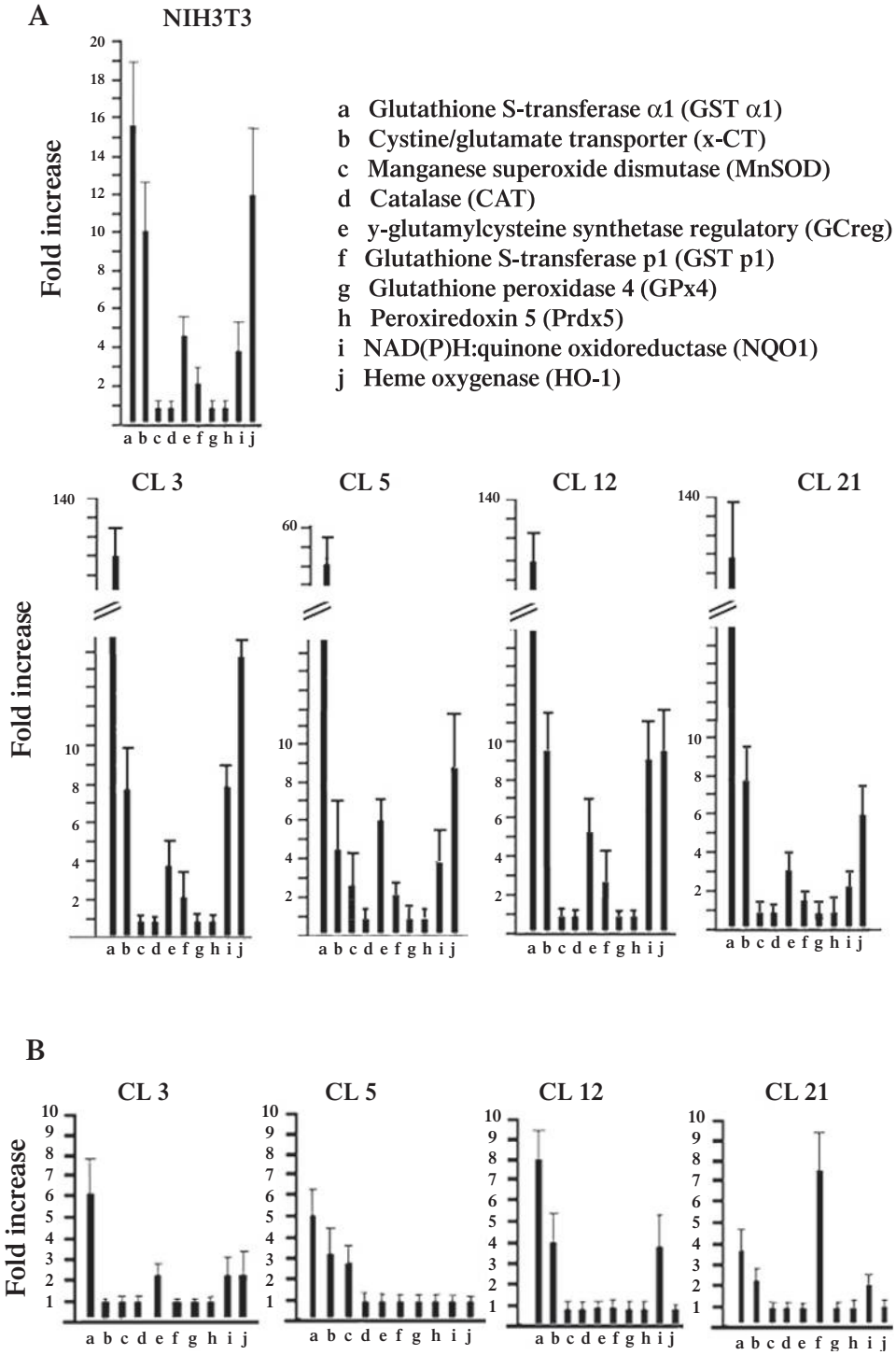

FIG. 4. Expression profile of antioxidant-response genes in NIH3T3-DEM clones. (**A**) mRNA levels of antioxidant-response genes after treatment with 100 μ*M* DEM for 3 h of wild-type NIH3T3 cells and of NIH-DEM clones growth for 30 days in the absence of DEM. (**B**) mRNA levels of antioxidant genes in NIH-DEM clones grown for 30 days in the absence of DEM. The comparison of mRNA levels of antioxidant genes in (**A**) and (**B**) is relative to wild-type NIH3T3, giving to the level observed in these cells the value 1.

pression levels of some of the genes continued to be higher than those observed in wild-type cells even in the absence of the oxidative stress. Interestingly, the four clones showed significant differences among their expression profiles. In fact, while GST α1 mRNA is invariantly higher than in normal NIH3T3 cells, ranging from 3.7-fold in NIH-DEM-21 to 8.2-

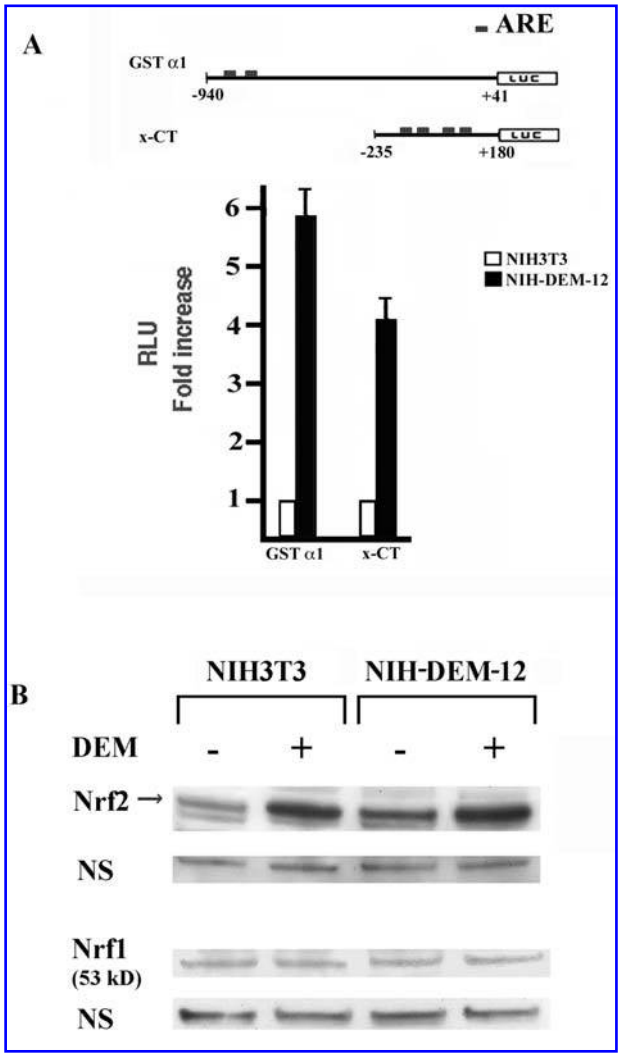

FIG. 5. Transcriptional regulation in NIH-DEM-12. (**A**) The promoters of GSTα1 (from −940 to +41) and x-CT (from −235 to +180) genes were amplified by PCR from mouse genomic DNA and cloned in PGL3 Basic vectors. The localization of putative ARE motifs is indicated. NIH3T3 and NIH-DEM-12 were transiently transfected with the reporter plasmids (5 μg) and pRLSV40 encoding Renilla luciferase (0.5 μg). At 36 h post-transfection, cells were harvested and analyzed for luciferase activity as described in Materials and Methods. The rate of induction was reported as fold induction relative to the wild-type NIH3T3 cells, which was set equal to 1 (RLU = relative luciferase units). The results are representative of three various independent experiments. (**B**) Western blot analysis of Nrf2 and Nrf1 protein in NIH3T3 cells and NIH-DEM-12. Nuclear proteins from NIH3T3 cells and NIH-DEM-12 treated with 100 μ*M* DEM for 3 h were extracted as described in Materials and Methods and 20 μg aliquots were resolved by SDS-PAGE. The Western blotting was performed with the antibodies specific for Nrf2 or Nrf1. A nonspecific band (NS) was used as reference.

fold in NIH-DEM-12, the other genes were either normal or increased in the four clones. In particular, NIH-DEM-21 which showed the lowest level of GST α1, is the only clone where we found high levels of GST p1 mRNA. On the contrary, NIH-DEM-5 cells are characterized by a sustained expression of MnSOD mRNA, whose levels are absolutely normal in all the other clones. Furthermore, the mRNA of cystine/glutamate transporter x-CT is increased in all the examined clones but not in NIH-DEM-3.

The comparison of these results with those shown in Figure 2B suggests that higher levels of GST α1 and x-CT mRNAs seem to be associated with the highest resistance to the DEM-induced stress, while GST p is not as effective as GST α1 to counteract GSH depletion provoked by DEM, at least in the experimental conditions used.

Transcription regulation of GST α1 and x-CT in NIH3T3 resistant to DEM

The understanding of the mechanisms underlying the sustained expression of antioxidant-response genes, even 1 month after the withdrawal of the drug from the culture medium, could be of help to explore the general mechanisms responsible for the development of the DEM-resistant phenotype in NIH3T3 cells. Therefore, we addressed the reasons for the high basal levels of GST α1 and x-CT mRNAs, observed in the NIH-DEM-12. It is well demonstrated that the regulation of transcription of specific genes plays a key role in the cellular response to an acute oxidative stress (12). Antioxidant-response elements (ARE) are present in numerous gene promoters, including those of GST α1 and x-CT, and are responsible for the activation of the transcription as a consequence of the oxidative stress (8, 17). In this view we generated two luciferase reporter constructs containing 940 and 235 bp upstream of the transcription start sites of these two genes, respectively. These two vectors were transfected in wild-type NIH3T3 and in NIH-DEM-12 grown in normal medium. As shown in Figure 5A, the expression levels driven by these vectors were significantly higher in NIH-DEM cells than in wild-type NIH3T3, thus suggesting that the DEM-resistant cells express a trans-acting factor which affects the transcription from the two endogenous gene promoters and then is responsible for the observed accumulation of the two mRNAs.

ARE are known to interact with the transcription factor Nrf2. This protein is regulated by Keap 1 factor which keeps Nrf2 sequestered in the cytoplasm. Upon the exposure of the cells to an oxidative stress, Nrf2 dissociates from Keap 1 and accumulates into the nucleus where it activates the transcription of the target genes (11). We measured the mRNA levels of Nrf2 and Keap 1 in wild-type and NIH-DEM-12 cells, but we failed to find any significant difference. On the contrary, the amount of Nrf2 protein, measured by Western blot in nuclear extracts from NIH-DEM-12 cells, was higher than that detected in NIH3T3 cells (see Fig. 5B). Furthermore, the accumulation of Nrf2 in the nuclei of DEM-resistant cells upon the exposure to 100 μ*M* DEM was significantly higher than that observed in the wild-type cells under the same conditions.

DISCUSSION

In this study we have analyzed the molecular phenotypes of NIH3T3-derived clones and selected for their ability to survive prooxidant conditions induced by the glutathione depletion. The analysis of the expression profiles of several genes involved in antioxidant defense mechanisms showed

that the resistance to DEM-induced oxidative stress, in all the examined clones, is invariantly associated with a dramatic increased expression of the glutathione *S*-transferase α1 gene, whose mRNA accumulates to concentrations 120-fold higher than those observed under basal conditions upon the exposure to DEM. This gene is clearly induced also in wild-type NIH3T3 cells, but this increase (about 15-fold) is not sufficient to prevent these cells from dying as a consequence of the DEM-induced stress. On the contrary, the induction of expression observed in DEM-resistant clones is sufficient to protect the cells from oxidative insults, even if the concentrations of DEM used are several-fold higher (up to 400 μ*M* instead of 100 μ*M*). These observations suggest that glutathione *S*-transferase α1 plays a key role in the anti-DEM defense mechanisms, and that there is a threshold for this enzyme activity below which the cells are not protected from DEM. It is well known that the alpha class GSTs can provide protection against electrophilic xenobiotics or drugs not only via their conjugation to GSH, but also by alleviating oxidative stress and subsequent lipid peroxidation that is often associated with exposure to xenobiotics (18). Overexpression of alpha class GSTs also protects the cells against various apoptosis-inducing stimuli, and this observation is in agreement with the finding that NIH-DEM clones show a robust resistance to apoptosis induced by UV, etoposide, and BSO.

The mechanisms underlying this prompt and dramatic accumulation of GST α1 mRNA in DEM-resistant clones appear to be based on the transcription of the cognate gene. In fact, a reporter construct in which the GST α1 gene promoter drives the expression of the luciferase gene, is induced more robustly in the NIH-DEM clones than in wild-type cells. The reason for this increased gene inducibility is probably related to the high basal levels of Nrf2 in the clones, and also to an increased sensitivity of the Nrf2 regulatory mechanisms to the oxidative stress. Our results clearly indicate that the increased levels of Nrf2 do not depend on an increased Nrf2 gene expression, as its mRNA levels are unchanged. One possible explanation for Nrf2 accumulation is that the protein is stabilized: the study of the mechanisms of this stabilization could reveal a further regulatory system of the antioxidant response. However, the simple increase of the Nrf2 levels is probably not sufficient to explain the observed induction of expression of GST α1 in NIH-DEM clones, that is also due to an increased sensitivity of the Nrf2 system to the oxidative stress. It is well known that Nrf2 is regulated by Keap1 (3), which restricts Nrf2 in the cytosol. We examined the levels of this regulatory protein and did not find any significant change, thus supporting the hypothesis that NIH-DEM clones have an enhanced efficiency of the Keap1-Nrf2 system or that also other transcription activator are induced in the examined clones.

Another characteristic of the NIH-DEM clones is the elevated expression of several antioxidant-response genes even in basal conditions. Surprisingly, the expression profiles vary among the four clones we examined in detail. In fact, while GST α1 gene expression is increased in all the examined clones, GST p1 gene is expressed at high levels only in the NIH-DEM-21 clone and MnSOD accumulates only in the NIH-DEM-5 clone. This last clone does not express high levels of NQO1 mRNA, which is on the contrary overexpressed in the other three clones. This variability suggests that, further to the induction of GST α1, likely regulated by the Nrf2 system, other gene expression programs could be activated in the same cell type to counteract chronic pro-oxidant conditions. Furthermore, the Nrf2-dependent activation of gene transcription does not seem to function to the same extent in all the examined clones. In fact, the x-CT gene, whose transcription is under the control of four AREs and thus is expected to be dependent on Nrf2, is not overexpressed in basal conditions in the NIH-DEM-3 clone. Taken together these results support the hypothesis that also other transcription factors regulate the antioxidant response and could be responsible for the sustained expression of defense genes in DEM-resistant cell clones.

ACKNOWLEDGMENTS

This work was supported by grants from Ministero dell' Università e della Ricerca Scientifica e Tecnologica (PRIN 2002 and PRIN 2004) and from Finanziamento Regione Campania L.R. 5/2003.

ABBREVIATIONS

ARE, antioxidant responsive element; BSO, buthionine sulfoximine; CAT, catalase; x-CT, cystine/glutamate transporter; DEM, diethylmaleate; DTT, 1,4-dithiothreitol; EDTA, ethylenediaminetetraacetic acid; GCreg, γ-glutamylcysteine synthetase regulatory; GPx, glutathione peroxidase; GST, glutathione *S*-transferase; HO-1, heme oxygenase; MnSOD, manganese superoxide dismutase; NQO1, NAD(P)H:quinone oxidoreductase-1; Nrf2, NF-E2-related factor; PMSF, phenylmethylsulfonyl fluoride; PI, propidium iodide; Prdx, peroxiredoxin; ROS, reactive oxygen species; TUNEL, terminal deoxynucleotidyl transferase (TdT)-mediated dUTP nick-end labeling.

REFERENCES

1. Dhakshinamoorthy S and Jaiswal AK. Functional characterization and role of INrf2 in antioxidant response element-mediated expression and antioxidant induction of NAD(P)H:quinone oxidoreductase1 gene. *Oncogene* 20: 3906–3917, 2001.
2. Dhakshinamoorthy S, Long DJ 2nd, and Jaiswal AK. Antioxidant regulation of genes encoding enzymes that detoxify xenobiotics and carcinogens. *Curr Top Cell Regul* 36: 201–216, 2000.
3. Dinkova-Kostova AT, Holtzclaw WD, Cole RN, Itoh K, Wakabayashi N, Katoh Y, Yamamoto M, and Talalay P. Direct evidence that sulfhydryl groups of Keap1 are the sensors regulating induction of phase 2 enzymes that protect against carcinogens and oxidants. *Proc Natl Acad Sci USA* 99: 11908–11913, 2002.
4. Droge W. Free radicals in the physiological control of cell function. *Physiol Rev* 82: 47–95, 2002.
5. Esposito F, Ammendola R, Faraonio R, Russo T, and Cimino F. Redox control of signal transduction, gene ex-

pression and cellular senescence. *Neurochem Res* 29: 617–628, 2004.
6. Finkel T and Holbrook NJ. Oxidants, oxidative stress and the biology of ageing. *Nature* 408: 239–247, 2000.
7. Finkel T. Oxidant signals and oxidative stress. *Curr Opin Cell Biol* 15: 247–254, 2003.
8. Friling RS, Bensimon A, Tichauer Y, and Daniel V. Xenobiotic-inducible expression of murine glutathione *S*-transferase Ya subunit gene is controlled by an electrophile-responsive element. *Proc Natl Acad Sci USA* 87: 6258–6262, 1990.
9. Griffith OW and Meister A. Potent and specific inhibition of glutathione synthesis by buthionine sulfoximine (*S-n*-butyl homocysteine sulfoximine). *J Biol Chem* 254: 7558–7560, 1979.
10. Hunt CR, Sim JE, Sullivan SJ, Featherstone T, Golden W, Von Kapp-Herr C, Hock RA, Gomez RA, Parsian AJ, and Spitz DR. Genomic instability and catalase gene amplification induced by chronic exposure to oxidative stress. *Cancer Res* 58: 3986–3992, 1998.
11. Itoh K, Wakabayashi N, Katoh Y, Ishii T, Igarashi K, Engel JD, and Yamamoto M. Keap1 represses nuclear activation of antioxidant responsive elements by Nrf2 through binding to the amino-terminal Neh2 domain. *Genes Dev* 13: 76–86, 1999.
12. Jaiswal AK. Regulation of antioxidant response element-dependent induction of detoxifying enzyme synthesis. *Methods Enzymol* 378: 221–238, 2004.
13. Livak KJ and Schmittgen TD. Analysis of relative gene expression data using real-time quantitative PCR and the 2(-Delta Delta C(T)) method. *Methods* 25: 402–408, 2001.
14. Ma W, Li D, Sun F, Kleiman NJ, and Spector A. The effect of stress withdrawal on gene expression and certain biochemical and cell biological properties of peroxide-conditioned cell lines. *FASEB J* 18: 480–488, 2004.
15. Pelicano H, Carney D, and Huang P. ROS stress in cancer cells and therapeutic implications. *Drug Resist Updat* 7: 97–110, 2004.
16. Pervaiz S and Clement MV. Tumor intracellular redox status and drug resistance—serendipity or a causal relationship? *Curr Pharm Des* 10: 1969–1977, 2004.
17. Sasaki H, Sato H, Kuriyama-Matsumura K, Sato K, Maebara K, Wang H, Tamba M, Itoh K, Yamamoto M, and Bannai S. Electrophile response element-mediated induction of the cystine/glutamate exchange transporter gene expression. *J Biol Chem* 277: 44765–44771, 2002.
18. Sharma R, Yang Y, Sharma A, Awasthi S, and Awasthi YC. Antioxidant role of glutathione *S*-transferases: protection against oxidant toxicity and regulation of stress-mediated apoptosis. *Antioxid Redox Signal* 6: 289–300, 2004.
19. Simon HU, Haj-Yehia A, and Levi-Schaffer F. Role of reactive oxygen species (ROS) in apoptosis induction. *Apoptosis* 5: 415–418, 2000.
20. Tome ME and Briehl MM. Thymocytes selected for resistance to hydrogen peroxide show altered antioxidant enzyme profiles and resistance to dexamethasone-induced apoptosis. *Cell Death Differ* 8: 953–961, 2001.
21. Toussaint O, Royer V, Salmon M, and Remacle J. Stress-induced premature senescence and tissue ageing. *Biochem Pharmacol* 64: 1007–1009, 2002.
22. Wasserman WW and Fahl WE. Functional antioxidant responsive elements. *Proc Natl Acad Sci USA* 94: 5361–5366, 1997.
23. Yang Y, Sharma A, Sharma R, Patrick B, Singhal SS, Zimniak P, Awasthi S, and Awasthi YC. Cells preconditioned with mild, transient UVA irradiation acquire resistance to oxidative stress and UVA-induced apoptosis: role of 4-hydroxynonenal in UVA-mediated signaling for apoptosis. *J Biol Chem* 278: 41380–41388, 2003.

Address reprint requests to:
Prof. Filiberto Cimino
Dipartimento di Biochimica e Biotecnologie Mediche
Università di Napoli Federico II
Via S. Pansini 5
80131 Napoli, Italy

E-mail: cimino@dbbm.unina.it

Received after revision September 20, 2005; accepted September 21, 2005.

This article has been cited by:

1. P Indovina, F Giorgi, V Rizzo, B Khadang, S Schenone, D Di Marzo, I M Forte, V Tomei, E Mattioli, V D'Urso, B Grilli, M Botta, A Giordano, F Pentimalli. 2011. New pyrazolo[3,4-d]pyrimidine SRC inhibitors induce apoptosis in mesothelioma cell lines through p27 nuclear stabilization. *Oncogene* . [CrossRef]
2. M Lo, V Ling, Y Z Wang, P W Gout. 2008. The xc- cystine/glutamate antiporter: a mediator of pancreatic cancer growth with a role in drug resistance. *British Journal of Cancer* **99**:3, 464-472. [CrossRef]
3. Vittorio Calabrese , Mahin D. Maines . 2006. Antiaging Medicine: Antioxidants and Aging. *Antioxidants & Redox Signaling* **8**:3-4, 362-364. [Citation] [Full Text PDF] [Full Text PDF with Links]